Slow Magnetic Relaxation and Single-Molecule Toroidal Behaviour in a Family of Heptanuclear {$Cr^{III}Ln^{III}_6$} (Ln = Tb, Ho, Er) Complexes

Kuduva R. Vignesh, Stuart K. Langley, Abinash Swain, Boujemaa Moubaraki,
Marko Damjanović, Wolfgang Wernsdorfer, Gopalan Rajaraman,* and Keith S. Murray*

Dedicated to Professor Peter Comba on the occasion of his 65th birthday

Abstract: *The synthesis, magnetic properties, and theoretical studies of three heterometallic {$Cr^{III}Ln^{III}_6$} (Ln = Tb, Ho, Er) complexes, each containing a metal topology consisting of two Ln_3 triangles connected via a Cr^{III} linker, are reported. The {$CrTb_6$} and {$CrEr_6$} analogues display slow relaxation of magnetization in a 3000 Oe static magnetic field. Single-crystal measurements reveal opening up of the hysteresis loop for {$CrTb_6$} and {$CrHo_6$} molecules at low temperatures. Ab initio calculations predict toroidal magnetic moments in the two Ln_3 triangles, which are found to couple, stabilizing a con-rotating ferrotoroidal ground state in Tb and Ho examples and extend the possibility of observing toroidal behaviour in non Dy^{III} complexes for the first time.*

$\mathbf{L}$anthanide complexes of the {Dy_3} triangular type continue to create great interest from experimental and theoretical perspectives, because of their single-molecule toroidal moment (SMT) properties.[1,2] Toroidal magnetic behaviour has thus far been observed with complexes having anisotropic ions owing to the non-collinear arrangement of the spins.[2] If two molecular triangles exhibiting toroidal states are connected via a linker, such as a 3d ion, then this offers the possibility of observing coupling between the two toroidal moments resulting in ferrotoroidicity, which can be utilized for the design of molecule-based multiferroics.[3] Recently, we have discovered a heterometallic heptanuclear complex of type {$Cr^{III}Dy^{III}_6$} in which two Dy^{III}_3 triangles are linked by an octahedral Cr^{III} ion.[4] This compound is the first species to display a ferrotoroidal moment in the ground state brought about by con-rotation (rotate in the same direction) of the local {Dy_3} toroidal quantum states. While toroidal and ferrotoroidal systems have been detailed for Dy^{III} ions, this behaviour has not been confirmed for other lanthanide ions as a variation in the orientation of the g-anisotropy is expected. Particularly if the ground-state electron density of the lanthanide ion is switched from oblate to prolate then this may have a significant consequence on the expected toroidicity. Therefore, a key question in regard to the heptanuclear compound was whether the Ln^{III} centres could be modified to identify if other Ln^{III}_3 triangles would show slow magnetic relaxation, toroidal moments, and ferrotoroidicity.

Herein we describe the variation in the Ln^{III} ion and provide a detailed analysis of the magnetic properties. The reported complexes have molecular formulae of [$Cr^{III}Ln^{III}_6$-$(OH)_8(o\text{-tol})_{12}(NO_3)(MeOH)_5$]$\cdot$ 2MeOH (Ln = Tb(**1**), Ho(**2**) and Er(**3**), $o\text{-tol} = o$-toluate) and we reveal that **1** and **2** display con-rotation of the local Ln_3 toroidal moments in the ground state, while the local Ln_3 toroidal moment is absent for **3**.

Single-crystal X-ray analysis reveals that **1**–**3** are isostructural, crystallizing in the triclinic space group, $P\bar{1}$ (see the Supporting Information, Table S1 for full crystallographic details). Each complex contains a heptanuclear core consisting of a single Cr^{III} ion and six Ln^{III} ions (Figure 1 for **1** and the Supporting Information, Figure S1 for **2** and **3**). The asymmetric unit contains half the complex, (three Ln^{III} ions and one half of the Cr^{III} ion) with the Cr^{III} ion lying upon an inversion centre. The ligand coordination is as described previously for {$Cr^{III}Dy^{III}_6$}[4] (see the Supporting Information, Table S2 for relevant structural parameters).

The room temperature $\chi_M T$ values (χ_M = the molar magnetic susceptibility) for **1**–**3** are 68.95, 86.32, and 67.25 $cm^3 K\,mol^{-1}$, respectively (Figure 2; Supporting Information, Figure S2). These values are in good agreement with the calculated values (70.9 (**1**), 86.3 (**2**), and 72.8 (**3**) $cm^3 K\,mol^{-1}$) for one Cr^{III} and six Ln^{III} non interacting

[*] Dr. K. R. Vignesh
 IITB-Monash Research Academy, IIT Bombay
 Powai, Mumbai, Maharashtra, 400076 (India)

 Dr. S. K. Langley
 School of Science and the Environment, Division of Chemistry,
 Manchester Metropolitan University
 Manchester (UK)

 A. Swain, Prof. G. Rajaraman
 Department of Chemistry, Indian Institute of Technology Bombay
 Powai, Mumbai, Maharashtra, 400 076 (India)
 E-mail: rajaraman@chem.iitb.ac.in

 Dr. B. Moubaraki, Prof. K. S. Murray
 School of Chemistry, Monash University
 Clayton, Victoria, 3800 (Australia)
 E-mail: keith.murray@monash.edu

 Dr. M. Damjanović, Prof. W. Wernsdorfer
 Institute Néel, CNRS, Université Grenoble Alpes, 25 rue des Martyrs,
 F-38000 Grenoble, France
 and
 Institute of Nanotechnology (INT), Karlsruhe Institute of Technology
 (KIT), Hermann-von-Helmholz-Platz 1
 76344 Eggenstein-Leopoldshafen (Germany)

 Supporting information (experimental, crystallography and compu-
 tational details (anisotropy values) and SQUID (ac data and other
 plots)) and the ORCID identification number(s) for the author(s) of
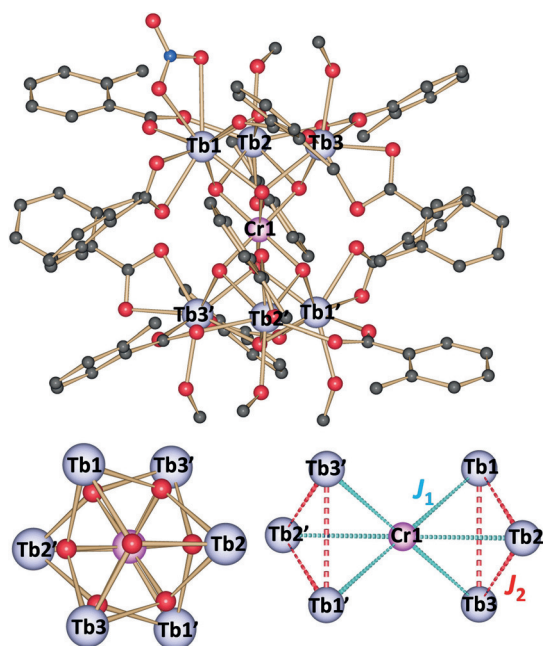 this article can be found under:
 https://doi.org/10.1002/anie.201711844.

Figure 1. Top: Molecular structure of complex **1**. The solvent and H atoms are omitted for clarity. Cr^{III} pink, Tb^{III} violet, O red, N blue, C light grey. Bottom left: Top view of metal topology found in **1**–**3**. Bottom right: Magnetic exchange pathways in J_1, and J_2 highlighted.
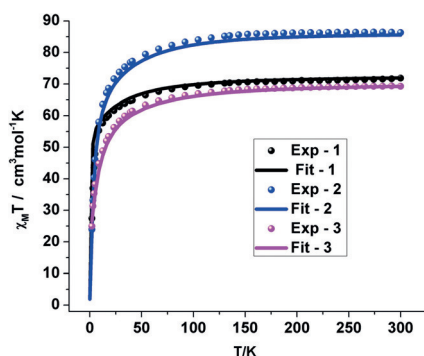

Figure 2. The measured (circles) and the fitted (solid lines) $\chi_M T$ values of complexes **1** (CrTb$_6$), **2** (CrHo$_6$), and **3** (CrEr$_6$). The measured data are up scaled by 4.0% and 3.0% for **1** and **3**, respectively.

ions. In each case, $\chi_M T$ declines with lowering temperature that is mainly due to single ion crystal-field effects and weak magnetic exchange effects (see later for analysis).

Magnetisation (M) isotherms against magnetic field (H) reach values of 28 (**1**), 36 (**2**), and 30 $N\beta$ (**3** at 2 K and 5 T, without saturation in M, the shapes being indicative of low lying, closely spaced energy levels being thermally populated (Supporting Information, Figure S3). We note that the S-shaped dependence of M vs. H,

at 2 K, which is characteristic (but not always seen)[3c] for a molecule possessing a toroidal magnetic moment[1,2] was not observed in these cases (see the Supporting Information, Figure S4 for low field M).

To check for slow magnetisation reversal (that is, possible SMM behaviour), ac susceptibility measurements were performed. No out-of-phase signal was found for **1**–**3** in the absence of a static dc magnetic field. However, in an optimum dc field of 3000 Oe, frequency dependent maxima were clearly evident below about 4 K for **1** (Supporting Information, Figure S5, left) and **3** (Figure 3, left) indicative of field induced SMM behaviour (no signal observed for **2**). The Cole–Cole plots between 1.8 K to 4 K suggest two relaxation processes for both **1** and **3** (Figure 3, right; Supporting Information, Figure S5, right). Fitting the data allowed for the extraction of the relaxation times and an Arrhenius plot ($\ln(\tau)$ vs. T^{-1}) yielded; $U_{eff} = 12.3$ K and $\tau_o = 6.3 \times 10^{-8}$ s for **1** and $U_{eff} = 4.5$ K and $\tau_o = 9.1 \times 10^{-8}$ s for **3** for the temperature-dependent process.[5] The second process in each case is found to be nearly temperature-independent, thus indicative of relaxation via quantum tunnelling of the magnetization (QTM; Supporting Information, Figure S6). We are aware that variations in the dc bias field can lead to different relaxation mechanisms becoming operative including inter-molecular effects and dilution studies were in part aimed to check this.[6] Measurements on magnetically dilute samples **1d**–**3d** (10% paramagnetic ion in a diamagnetic {AlLu$_6$} matrix; see the Supporting Information for details) were also performed using the same dc bias field. Interestingly, we find the relaxation times increase for **1d** yet decrease for **3d** (Supporting Information, Figures S8 and S9). No out-of-phase signal is again observed for **2d**.

Micro-SQUID measurements on single crystals of **1**–**3** were studied at many temperatures and sweep rates.[7] When the field is applied between the {Ln^{III}$_3$} triangles along the Ln–Ln bond hysteresis is observed below 0.03 K for **1** (CrTb$_6$) and **2**(CrHo$_6$) but not for **3** (CrEr$_6$; Figure 4; Supporting Information, Figures S10–S12), with the coercive field widening on cooling (H$_c$ = 0.4 T at 0.03 K, with a sweep rate of 0.14 T s^{-1}). Comparing these data to the {CrDy$_6$} analogue[4] we find the absence of steps at a particular magnetic field indicative of toroidal behaviour. As both the Ho^{III} and Tb^{III} species are
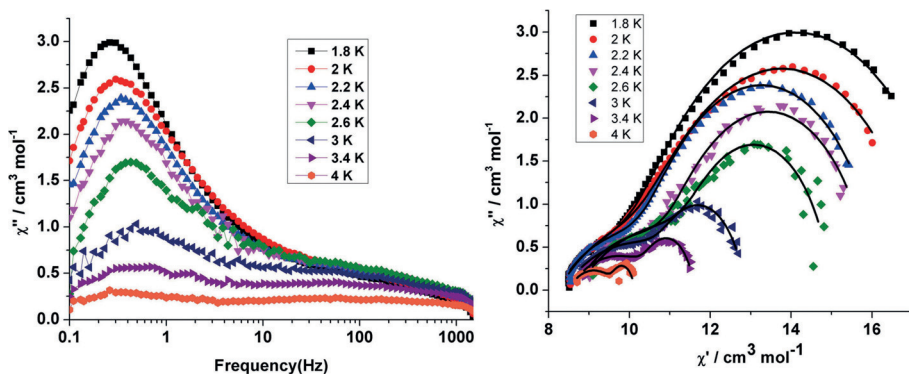

Figure 3. Left: Frequency dependence of χ_M'' for **3** in a 3000 Oe applied dc field, with an ac magnetic field of 3.5 Oe. Right: Cole–Cole plots between 1.8–4 K. The black lines are fits of the data using CC-fit.[5]
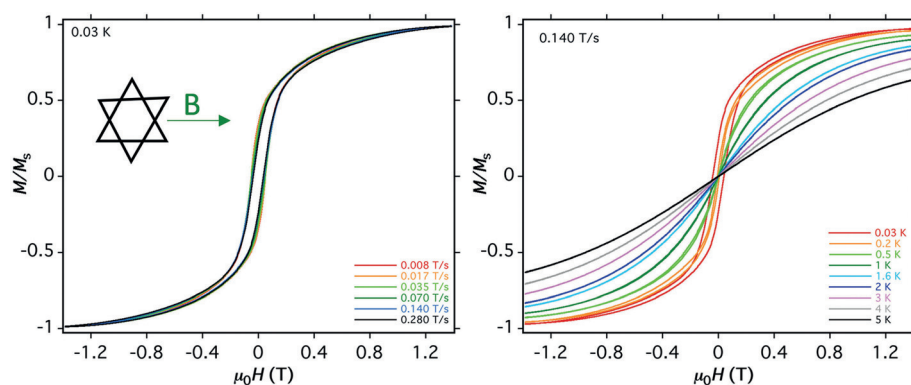
Figure 4. Left: Single-crystal magnetization (*M*) vs. applied field measurements (μ-SQUID) for complex **2** with different field sweep rates at 0.03 K. Inset: the applied field direction through Ln—Ln bond. Right: *M* vs. applied field with the scan rate of 0.14 Ts^{-1} from 0.03 K to 5 K.

non-Kramers in nature, greater tunnelling between the levels is expected and this could perhaps mask the expected steps in the single crystal measurements. This suggests that further detailed studies such as NMR are needed to prove/disprove the predicted SMT behaviour by means of ab initio methods (see below). Complex **2** shows wider coercivity compared to complex **1** and this is mainly attributed to the difference in the computed magnetic exchange states (see theoretical section below).

We performed ab initio CASSCF calculations on **1–3** with MOLCAS 8.0[8] (see the Supporting Information for details), a method that is successful in interpreting the magnetism of lanthanide complexes.[1g, 9] We have probed a) the single ion anisotropy of all ions; b) the Cr-Ln exchange;; c) the dipolar interaction between nearest Ln^{III}–Ln^{III} and Cr^{III}–Ln^{III} ions, and d) the toroidal magnetic moment.

The results of the single ion analysis are shown in the Supporting Information, Tables S7–S9. The orientation of the main anisotropy axes in the Ising doublets of **1** and **2** and the ground KDs for **3** are shown in Figure 5 and the Supporting Information, Figure S13, respectively. The calculations indicate that no slow magnetic relaxation should be observed in the absence of an applied dc magnetic field, due to QTM, as is
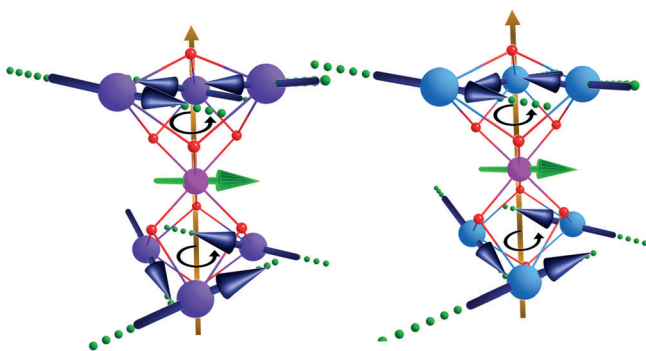
observed experimentally. Owing to the large ground-to-first excited state energy gap, however, our analysis suggests that the application of a static dc field is expected to quench the QTM between the ground states for **1–3** and allow for slow magnetic relaxation. Upon application of a bias dc field we found this to be the case for **1** and **3**, but was inconclusive for **2**, which is possibly due to the very large tunnel splitting compared to **1** (Supporting Information, Figure S6). This was further corroborated from the dilution experiments, which better simulate the single ion cases experimentally. The presence of large QTM/tunnel splitting is supported by the CF parameters. In **1–3**, the non-axial (in which $q \neq 0$ and $k = 2, 4, 6$) terms are larger than the axial terms (in which $q = 0$ and $k = 2, 4, 6$) suggesting prominent QTM effects in the ground states (Supporting Information, Tables S10 and S11).[9c] The magnitudes of the CF parameters of Tb are large compared to Ho and this is mainly due to the diminishing nature of oblate characteristics from Tb to Ho.[10]

Using the POLY ANISO[11] program the exchange/dipolar interactions between Cr^{III}-Ln^{III} (J_1) and nearest-neighbour Ln^{III} (J_2) sites are computed and tabulated in Table 1 (see

Table 1: Computed exchange and dipolar couplings [cm^{-1}] of **1–3**.

Complex	J_1 (Cr^{III}–Ln^{III})			J_2 (Ln^{III}–Ln^{III})			zJ
	J_{exch}	J_{dip}	J_{tot}	J_{exch}	J_{dip}	J_{tot}	
1	−0.2	0.1	−0.1	−0.1	0.02	−0.08	−0.01
2	−0.18	−0.07	−0.25	0.5	0.1	0.6	−0.01
3	−1.0	−0.2	−1.2	−0.8	−0.05	−0.85	−0.04

computational details in the Supporting Information for the Hamiltonian used, and Figure 1, bottom right). By employing the calculated exchange parameters, good fits to both the susceptibility and the magnetization data were achieved for all complexes employing the Lines approach (Figure 2; Supporting Information, Figures S2, S3). We note the small angle ($\theta = 17.6°$) between the orientation of magnetic anisotropy and the vector connecting two Ho^{III} ions leads to ferromagnetic coupling.[12] Whereas in **1** and **3**, this angle (θ) is found to be larger (39.4° and 59.5°), and thus could contribute to the antiferromagnetic dipolar part of the exchange interactions. Among the three complexes the largest *J* values are calculated for **3** (Er^{III}), which has also been noted in other studies.[13] The Cr^{III}-Ln^{III} interactions for all three complexes are found to be antiferromagnetic in nature, which is in line with previous studies.[14] The ferromagnetic dipolar coupling between the lanthanide ions and the S_6 symmetry of the complexes in **1** and **2** induce the local magnetic moments on the Ln^{III} centres in the ground exchange state leading to

Figure 5. The direction of the local anisotropy axes in the ground Ising doublet on each Tb^{III} and Ho^{III} site (green dotted lines) in **1** and **2**, respectively. The straight blue arrows are the local magnetic moment in the ground exchange doublet. The black arrows show the con-rotation of the toroidal magnetic moment and the yellow/ arrow is the S_6 symmetry axis.

a net magnetic moment, similar to that observed for the analogous {Cr^{III}Dy$^{III}_6$}.[4]

In **1–3**, the QTM for the exchanged coupled ground state was computed to be small (0.67×10^{-1} (**1**), 0.21×10^{-1} (**2**), and 0.13×10^{-1} (**3**)), but the TA-QTM at the coupled first excited was found to be large (Figure 6; Supporting Information,
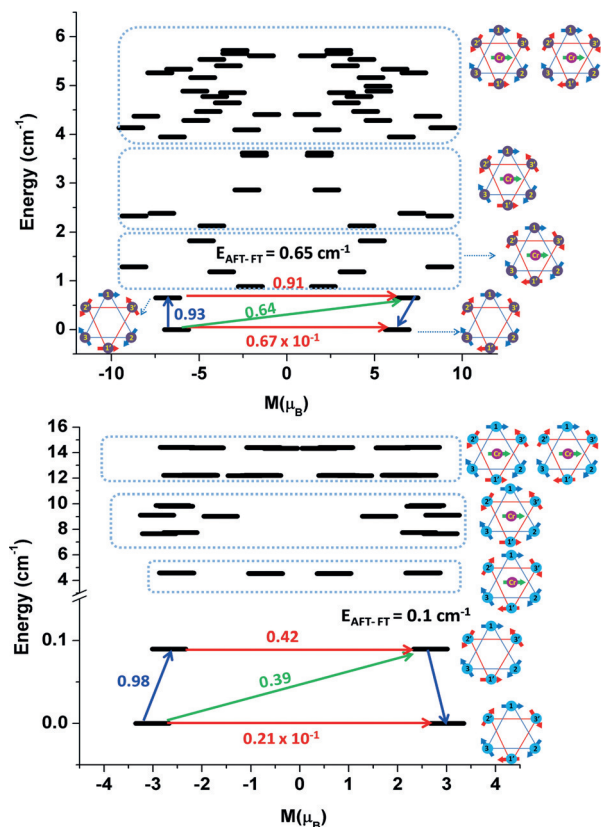

Figure 6. Low-lying exchange spectrum for **1** (top) and **2** (bottom). The exchange coupled states (KDs) are placed on the diagram according to their magnetic moments (bold black lines). The green/blue arrows show the possible pathway via Orbach/Raman relaxation. The solid red lines represent the presence of QTM/TA-QTM between the connecting KDs. For various energy states a graphical representation of one of the corresponding non-collinear Ising quantum states, where the red/blue thick arrows at the Ln^{III} sites indicate the direction of the magnetic moment in toroidal form. Note here that all the states represented for **1** and **2** are KDs as Tb^{III} and Ho^{III} non-Kramers states couple with $S = 3/2$ state of the Cr^{III} ion.

Figure S15). Thus, in **1–3** the magnetic relaxation occurs via the low-lying excited states with relatively smaller energy barriers. This again supports the lack of an out-of-phase signal for **1–3** at 2 K in zero dc field. The exchange coupled model again predicts that the application of a suitable field will quench the QTM among the lowest-lying states allowing for relaxation via higher excited states, as is observed. Moreover, in **3** a second relaxation is predicted at the excited state (Supporting Information, Figure S15, top) with an energy barrier of 3.5 cm^{-1} (5.0 K). This result is consistent with the experimental data (Figure 3). This relaxation process is mainly a consequence of the relatively strong Er^{III}···Er^{III} and

Cr^{III}···Er^{III} coupling that quenches the ground state QTM, allowing the relaxation to proceed via the third excited states.

The direction of the local anisotropy axes on all Ln sites are shown in Figure 5 and the Supporting Information, Figure S13 by dashed lines. For **1** and **2**, owing to the ferromagnetic dipolar coupling the direction of the spins along the main anisotropy axes on each Ln^{III} ion are following each other, thus forming a circular pattern in both Ln$_3$ triangles. Moreover, we calculate con-rotation between the two triangles, suggesting alignment of toroidal moments (a ferrotoroidal state, FT), as observed for the {Cr^{III}Dy$^{III}_6$} complex.[4] The toroidal moment is not predicted for **3**. Note here that the dipolar coupling included in the fit employed a well-known dipolar Hamiltonian where the magnetic moments of all the ions and their corresponding distances are taken into consideration [see Eq. (1) in Ref. [4]]. The ferrotoroidal ground state is essentially stabilized due to the strong dipolar interactions between the {Ln$_3$} rings and to affirm that the ground state is FT, we have simulated the magnetization data at 2 K for complexes **1** and **2** with and without the dipolar exchange. Exclusion of dipolar coupling results in the stabilization of an AFT (antiferrotoroidal) state and the simulated data deviate significantly from the experiments supporting the assignment of FT ground states for complexes **1** and **2**. (see the Supporting Information, Figures S16, S17 for the *M* vs. *H* data and the corresponding energy-level diagram). It should be noted here, however, both **1** and **2** possess non-Kramers ions, thus larger tunnel splittings are expected, which is reflected in the calculations. The larger tunnelling splitting between the states likely to lead to fast magnetic relaxation as witnessed in the single-crystal magnetic hysteresis measurements.

The orientation of the main anisotropic axis can be rationalised qualitatively based on the difference in electron density of the ground state m$_J$ levels among complexes **1–3**. As the electron density of the Tb^{III} and Ho^{III} ions are oblate in nature (equatorially expanded) and it is the μ_3-O ligands that possess the largest electrostatic charges, in order to minimize the electrostatic repulsion, the g_{zz} axis of each Tb^{III} and Ho^{III} ion lies along direction of the μ_3-O atoms, allowing for the electron density to lie perpendicular to the direction of the axes. This configuration results in the circular pattern and hence the toroidal moment. For **3**, however, the Er^{III} ion is prolate in nature and the electron density is axially elongated which causes the g_{zz} axis of each ion to lie perpendicular to the {Ln$_3$} triangle resulting in the absence of a circular pattern and, hence, no toroidal behaviour. The magnetic moments of the six Ln^{III} ions in the {Cr^{III}Tb$^{III}_6$} and {Cr^{III}Ho$^{III}_6$} complexes lead to a total magnetic moment of 16.3 μ_B and 13.1 μ_B, respectively, revealing a net toroidal magnetic moment in the ground state, compared to 13.9 μ_B for {Cr^{III}Dy$^{III}_6$}.[4] This result implies that the two toroidal moments rotate in the same direction, suggestive of ferrotoroidicity, whereas if they were to rotate in opposite directions the net toroidal moment would be about 0 μ_B.

Similar to our earlier studies on the {Cr^{III}Dy$^{III}_6$} complex,[4] we have analysed the inter-triangle dipolar-induced splitting between the FT ground state and the AFT first excited state and it is estimated to be 0.65 cm^{-1} for **1** and 0.1 cm^{-1} for **2**,

782 www.angewandte.org

© 2018 Wiley-VCH Verlag GmbH & Co. KGaA, Weinheim

Angew. Chem. Int. Ed. **2018**, *57*, 779 –784

compared to 0.28 cm^{-1} for {Cr^{III}Dy$^{III}_6$}. Here we note that the ground FT and AFT states possess a freely fluctuating Cr^{III} spin, while its direction is blocked in the excited states that lie beyond the FT/AFT states. The gap between the FT ground state and those states that lie beyond the FT/AFT states corresponds to the lowest magnetic excitation where one of the Ln^{III} spins needs to be flipped.[4] This energy is computed to be 4.5 cm^{-1} for complex **2** and it is 0.9 cm^{-1} for complex **1**. The larger gap computed for **2** is in agreement with the wider coercivity observed for complex **2** compared to complex **1** at 0.03 K in the single-crystal magnetic hysteresis measurements. As the dipolar coupling between the {Ln$^{III}_3$} triangles dominate the energy levels, the FT state is expected to be the ground state independent of the nature of Ln^{III}–Cr^{III} coupling. Such dipolar coupling interactions between lanthanide ions have been noted for several Dy^{III} based magnets.[14a, 15]

Thus, for the first time we have predicted toroidal behaviour in Tb^{III} and Ho^{III} systems; firstly, at the local {Ln$_3$} triangular level and, secondly, the local toroidal moments are found to couple in a con-rotating manner. Moreover, the ground state gap between the FT and AFT state is found to increase in {Cr^{III}Tb$^{III}_6$} (0.65 cm^{-1}), compared to {Cr^{III}Dy$^{III}_6$} (0.28 cm^{-1}),[4] but decreases for {Cr^{III}Ho$^{III}_6$} (0.1 cm^{-1}).

The inter-ring dipolar coupling between the Ln^{III} ions splits the FT and AFT states. As the magnitude of the exchange coupling estimated here is different compared to {CrDy$_6$}[4] and **1** possesses a somewhat larger J_{dip} value, this leads to the observation of a larger FT-AFT gap for **1** compared to the other complexes. This could also be qualitatively attributed to the stronger oblaticity exhibited by the m$_J$=±6 state of the Tb^{III} ion compared to the m$_J$=±8, m$_J$=±15/2 of Ho^{III} and Dy^{III} ions, respectively.

In summary, three heptanuclear {Cr^{III}Ln$^{III}_6$} (Ln = Tb (**1**), Ho (**2**), and Er (**3**)) complexes have been synthesised, structurally characterized, and magnetically and theoretically analysed for their SMM and SMT behaviour. The ab initio calculations are found to be in line with the experimental magnetic data, with **1–3** displaying SMM behaviour, only in the presence of an applied static dc field. Importantly, ab initio calculations suggest toroidal moment behaviour for the {Cr^{III}Tb$^{III}_6$} and {Cr^{III}Ho$^{III}_6$} complexes, with the ground toroidal state being the rotation of two toroidal moments in the same direction within the molecule. Moreover, we find an enhanced FT-AFT gap for **1** compared to the previously studied {CrDy$_6$} complex. This is the first time single molecule toroidal behaviour has been predicted for Tb and Ho systems, with the results indicating the likelihood of ferrotoroidicity, a rare and much sought after property in the design of multiferroic materials. Although the ab initio calculations with the proposed FT state reproduce the low-temperature magnetization successfully, strong experimental observations for such toroidicity is still lacking and further experiments to probe the toroidal behaviour using other techniques is underway in our laboratory.

Conflict of interest

The authors declare no conflict of interest.

[1] a) S.-Y. Lin, W. Wernsdorfer, L. Ungur, A. K. Powell, Y.-N. Guo, J. Tang, L. Zhao, L. F. Chibotaru, H.-J. Zhang, *Angew. Chem. Int. Ed.* **2012**, *51*, 12767–12771; *Angew. Chem.* **2012**, *124*, 12939–12943; b) A. Soncini, L. F. Chibotaru, *Phys. Rev. B* **2008**, *77*, 220406; c) J. Tang, I. Hewitt, N. T. Madhu, G. Chastanet, W. Wernsdorfer, C. E. Anson, C. Benelli, R. Sessoli, A. K. Powell, *Angew. Chem. Int. Ed.* **2006**, *45*, 1729–1733; *Angew. Chem.* **2006**, *118*, 1761–1765; d) L. Ungur, W. Van den Heuvel, L. F. Chibotaru, *New J. Chem.* **2009**, *33*, 1224–1230; e) D. Gatteschi, R. Sessoli, L. Sorace in *Handbook on the Physics and Chemistry of Rare Earths, Vol. 50* (Eds.: J.-C. G. Bünzli, V. K. Pecharsky.), Elsevier, Amsterdam, **2016**, pp. 91–139; f) J. Luzon, K. Bernot, I. J. Hewitt, C. E. Anson, A. K. Powell, R. Sessoli, *Phys. Rev. Lett.* **2008**, *100*, 247205; g) M. Gysler, F. El Hallak, L. Ungur, R. Marx, M. Hakl, P. Neugebauer, Y. Rechkemmer, Y. Lan, I. Sheikin, M. Orlita, C. E. Anson, A. K. Powell, R. Sessoli, L. F. Chibotaru, J. van Slageren, *Chem. Sci.* **2016**, *7*, 4347–4354.

[2] L. F. Chibotaru, L. Ungur, A. Soncini, *Angew. Chem. Int. Ed.* **2008**, *47*, 4126–4129; *Angew. Chem.* **2008**, *120*, 4194–4197.

[3] a) T. Kaelberer, V. A. Fedotov, N. Papasimakis, D. P. Tsai, N. I. Zheludev, *Science* **2010**, *330*, 1510–1512; b) G. Novitchi, G. Pilet, L. Ungur, V. V. Moshchalkov, W. Wernsdorfer, L. F. Chibotaru, D. Luneau, A. K. Powell, *Chem. Sci.* **2012**, *3*, 1169–1176; c) L. Ungur, S.-Y. Lin, J. Tang, L. F. Chibotaru, *Chem. Soc. Rev.* **2014**, *43*, 6894–6905.

[4] K. R. Vignesh, A. Soncini, S. K. Langley, W. Wernsdorfer, K. S. Murray, G. Rajaraman, *Nat. Commun.* **2017**, *8*, 1023.

[5] N. F. Chilton, *CC-fit model*, The University of Manchester.

[6] F. Habib, I. Korobkov, M. Murugesu, *Dalton Trans.* **2015**, *44*, 6368–6373.

[7] C. Cadiou, M. Murrie, C. Paulsen, V. Villar, W. Wernsdorfer, R. E. P. Winpenny, *Chem. Commun.* **2001**, 2666–2667.

[8] F. Aquilante, T. B. Pedersen, V. Veryazov, R. Lindh, *WIREs Comput. Mol. Sci.* **2013**, *3*, 143–149.

[9] a) S. K. Langley, N. F. Chilton, L. Ungur, B. Moubaraki, L. F. Chibotaru, K. S. Murray, *Inorg. Chem.* **2012**, *51*, 11873–11881; b) K. R. Vignesh, S. K. Langley, K. S. Murray, G. Rajaraman, *Chem. Eur. J.* **2017**, *23*, 1654–1666; c) K. R. Vignesh, S. K. Langley, K. S. Murray, G. Rajaraman, *Inorg. Chem.* **2017**, *56*, 2518–2532; d) C. Das, S. Vaidya, T. Gupta, J. M. Frost, M. Righi,

E. K. Brechin, M. Affronte, G. Rajaraman, M. Shanmugam, *Chem. Eur. J.* **2015**, *21*, 15639–15650; e) S. Biswas, S. Das, T. Gupta, S. K. Singh, M. Pissas, G. Rajaraman, V. Chandrasekhar, *Chem. Eur. J.* **2016**, *22*, 18532–18550.

[10] a) J. D. Rinehart, J. R. Long, *Chem. Sci.* **2011**, *2*, 2078–2085; b) T. Gupta, G. Velmurugan, T. Rajeshkumar, G. Rajaraman, *J. Chem. Sci.* **2016**, *128*, 1615–1630.

[11] L. F. Chibotaru, L. Ungur, Program POLY_ANISO **2006**, University of Leuven.

[12] J.-D. Leng, J.-L. Liu, W.-Q. Lin, S. Gomez-Coca, D. Aravena, E. Ruiz, M.-L. Tong, *Chem. Commun.* **2013**, *49*, 9341–9343.

[13] J. J. Le Roy, L. Ungur, I. Korobkov, L. F. Chibotaru, M. Murugesu, *J. Am. Chem. Soc.* **2014**, *136*, 8003–8010.

[14] a) S. K. Langley, D. P. Wielechowski, V. Vieru, N. F. Chilton, B. Moubaraki, B. F. Abrahams, L. F. Chibotaru, K. S. Murray, *Angew. Chem. Int. Ed.* **2013**, *52*, 12014–12019; *Angew. Chem.* **2013**, *125*, 12236–12241; b) K. S. Pedersen, G. Lorusso, J. J. Morales, T. Weyhermüller, S. Piligkos, S. K. Singh, D. Larsen, M. Schau-Magnussen, G. Rajaraman, M. Evangelisti, J. Bendix, *Angew. Chem. Int. Ed.* **2014**, *53*, 2394–2397; *Angew. Chem.* **2014**, *126*, 2426–2429.

[15] L. Ungur, S. K. Langley, T. N. Hooper, B. Moubaraki, E. K. Brechin, K. S. Murray, L. F. Chibotaru, *J. Am. Chem. Soc.* **2012**, *134*, 18554–18557.